JOURNAL OF SOLID STATE CHEMISTRY **136,** 284–292 (1998)
ARTICLE NO. SC977707

The Phase Transitions between $H_{0.27}V_{0.27}W_{0.73}O_3 \cdot \frac{1}{3}H_2O$ and $V_{0.27}W_{0.73}O_{2.865}$: An X-Ray, Thermal Analysis, and HREM Study

L. Dupont* and M. Sundberg†

*Laboratoire de Réactivité et de Chimie des Solides, UPRES A 6007, Université de Picardie Jules Verne, 33 rue Saint-Leu, F-80039 Amiens Cedex, France; and †Arrhenius Laboratory, Department of Inorganic Chemistry, Stockholm University, S-10691 Stockholm, Sweden

Received July 2, 1997; accepted November 17, 1997

A mixed vanadium–tungsten oxide hydrate ($H_{0.27}V_{0.27}W_{0.73}O_3 \cdot \frac{1}{3}H_2O$) has been synthesized by a soft chemistry method, and the phase transitions from the hydrate (precursor) to the final product $V_{0.27}W_{0.73}O_{2.865}$ have been studied by thermal analysis, X-ray powder diffraction, and high-resolution electron microscopy (HREM) techniques. Supermetastable, metastable, and stable oxides have been observed. $H_{0.27}V_{0.27}W_{0.73}O_3 \cdot \frac{1}{3}H_2O$ possesses a structure related to $WO_3 \cdot \frac{1}{3}H_2O$. Dehydration of the precursor leads to a supermetastable phase, $H_{0.27}V_{0.27}W_{0.73}O_3$, with a structure similar to that of the hydrate. At 350°C this phase transforms to the metastable $H_{0.27}V_{0.27}W_{0.73}O_3$, with a structure isotypic with WO_3(hex). The phase transition between the hydrate and $H_{0.27}V_{0.27}W_{0.73}O_3$ is both pseudomorphous and topotactic. Removal of hydrogen and oxygen from the metastable oxide induces a second phase transition at 500°C to a more stable phase, $V_{0.27}W_{0.73}O_{2.865}$, with an oxygen-deficient WO_3-type structure. The monoclinic symmetry of the latter oxide increases at higher temperature, first to orthorhombic and then to tetragonal. This transition is not pseudomorphous but of a topotactic nature. The obtained results suggest that the hydrogen content stabilizes the WO_3(hex)-related structure of the metastable phase. A hypothetical model based on HREM observations is proposed for the structural transformation $H_{0.27}V_{0.27}W_{0.73}O_3 \rightarrow V_{0.27}W_{0.73}O_{2.865}$.

INTRODUCTION

About two decades ago, tungsten trioxide hydrate, $WO_3 \cdot \frac{1}{3}H_2O$, was synthesized by Gerand *et al.* (1) by hydrothermal treatment at 120°C of an aqueous suspension of tungstic acid gel. Its structure, shown in Fig. 1a, can be described as consisting of infinite planar sheets of slightly distorted WO_6 octahedra, sharing corners to form six-membered rings. The sheets are stacked along the *c*-axis so that every second layer is shifted by *a*/2. Thermal treatment of the hydrate led to the formation of supermetastable (2), metastable, and stable (3) WO_3 phases with orthorhombic, hexagonal, and monoclinic structures, respectively. The orthorhombic supermetastable WO_3 phase is formed at 300°C by dehydration of the hydrate. The structure is isotypic with that of $WO_3 \cdot \frac{1}{3}H_2O$ in Fig. 1a. The supermetastable phase transforms to the hexagonal modification of WO_3 at 400°C. The latter structure (Fig. 1b) is built up of the same infinite sheets of corner-sharing octahedra as the hydrate but stacked instead as in the hexagonal tungsten bronze (HTB) structure (4). The hexagonal tunnels are empty in the WO_3(hex) structure but contain variable amounts of M^{1+} ions in the M_xWO_3 bronzes. At 500°C, WO_3(hex) transforms to the monoclinic modification of WO_3 with a distorted ReO_3-type structure (5) (Fig. 1c).

The concepts of structural filiation and metastability in soft chemistry have been developed by Figlarz (6). He used some examples from the chemistry of hexagonal WO_3 to illustrate the chemical transformation from the mother phase (precursor) to the daughter phase (the product of the transformation). It was pointed out that geometrical considerations of the mechanisms are probably not sufficient to prove the topotactic transformation. However, by using the powerful methods of selected-area electron diffraction (SAED) and high-resolution electron microscopy (HREM), it is possible to obtain direct structural information about the phase transformation going on in a crystal. By using these techniques, the mechanisms of nucleation and growth and the probable relationships between the hexagonal and the monoclinic WO_3 phases were found (7).

We have recently used a new preparation method (8) to synthesize a new mixed oxide hydrate, $H_{0.27}V_{0.27}W_{0.73}O_3 \cdot \frac{1}{3}H_2O$, isotypic with $WO_3 \cdot \frac{1}{3}H_2O$. It was precipitated from a solution of completely dissolved metallic tungsten and vanadium pentaoxide in 10% hydrogen peroxide. The experimental conditions for the formation and some first results from the characterization of the compound are given in ref 8.

It is interesting to note that Gopalakrishnan *et al.* (9) have prepared a related compound, $H_{0.33}V_{0.33}W_{0.67}O_3 \cdot 0.33H_2O$, by acid-leaching of $LiVWO_6$ with concentrated HNO_3. This mixed oxide hydrate is reported to be isostructural with $WO_3 \cdot \frac{1}{3}H_2O$, and it dehydrates to an anhydrous

0022-4596/98 $25.00

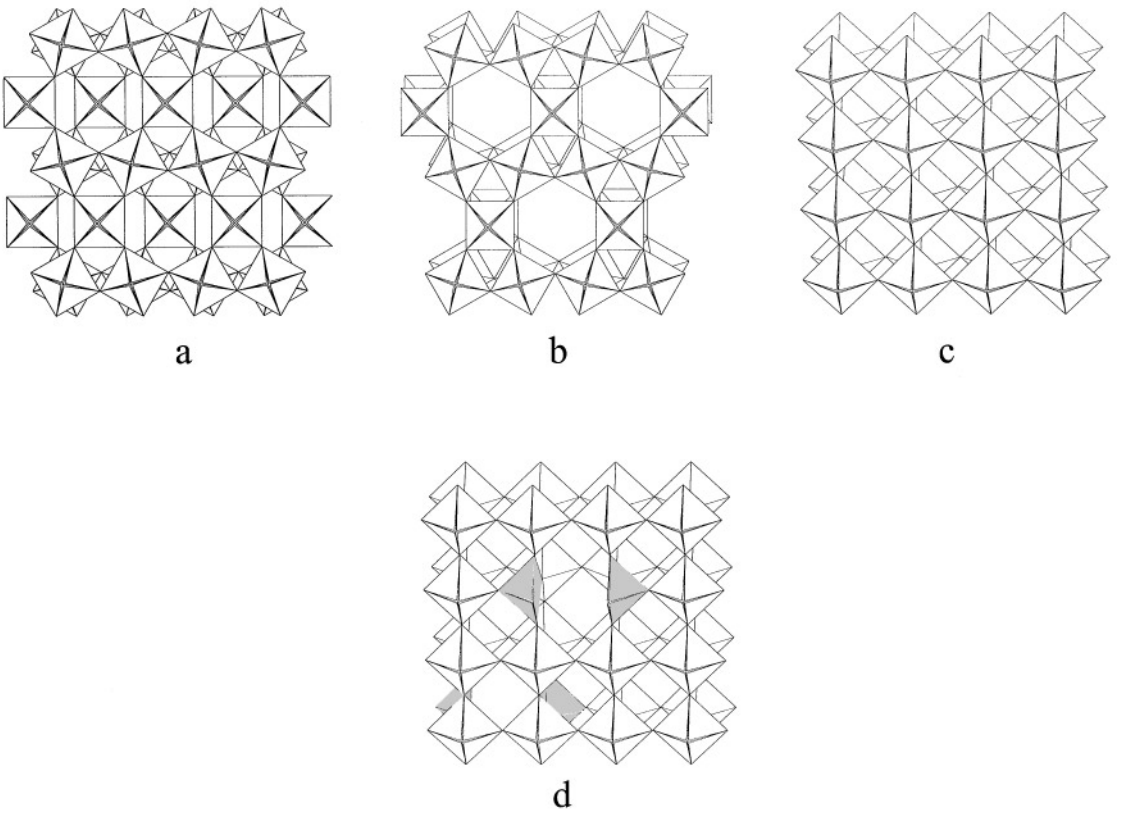

FIG. 1. Crystal structures of (a) $WO_3 \cdot \frac{1}{3}H_2O$, (b) WO_3(hex) in [001] projection, (c) WO_3(mon), and (d) V–W–oxide (oxygen-deficient ReO_3 type). The drawings were produced with ATOMS by Shape Software.

phase, $H_{0.33}V_{0.33}W_{0.67}O_3$, with a structure related to WO_3(hex).

The present paper describes how the phase transformations from the $H_{0.27}V_{0.27}W_{0.73}O_3 \cdot \frac{1}{3}H_2O$ precursor to the reaction product, $V_{0.27}W_{0.73}O_{2.865}$, have been elucidated by a combination of thermal analysis methods, X-ray diffraction, and HREM techniques.

EXPERIMENTAL

A description of the synthesis method has already been given in detail (8). X-ray diffraction studies were done with a Guinier–Lenne heating camera (Enraf diffractis 581, Cu monochromator, 0.1°/min, 1.5 mm/h). The X-ray results were supplemented with simultaneous thermal analysis: thermogravimetry (TG) and differential thermal analysis (DTA) on a Setaram TG-DTA 92 (5°/min).

For the electron microscopy study, a small amount of the particles were dispersed in 1-butanol by ultrasonic treatment. A drop of the suspension was collected on a holey carbon film supported on a Cu grid. The grids were studied in a JEOL JEM 200CX transmission electron microscope equipped with a top-entry, double-tilt goniometer stage ($\pm 10°$) and operated at 200 kV. The JEOL 200CX has a spherical aberration constant of 1.2 mm and a structural resolution limit of 2.4 Å. The electron micrographs were recorded at 320,000–430,000 times electron optical magnification. A TV camera with an image intensifier (LHESA MVN180) was used for focusing on the crystals at a low electron beam intensity.

RESULTS AND DISCUSSION

(A) X-Ray Diffraction and Thermal Analysis Studies

The X-ray powder diffraction data for $H_{0.27}V_{0.27}W_{0.73}O_3 \cdot \frac{1}{3}H_2O$ were indexed and used to refine the following orthorhombic unit cell parameters: $a = 7.276(1)$, $b = 12.575(2)$, and $c = 7.726(1)$ Å (8). The X-ray pattern resembles that of $WO_3 \cdot \frac{1}{3}H_2O$, with unit cell dimensions $a = 7.359$, $b = 12.513$, and $c = 7.704$ Å (1). The slight difference in the parameters can be explained by the difference in composition of the two compounds. The Guinier–Lenne X-ray photograph in Fig. 2 shows displacements and rearrangements

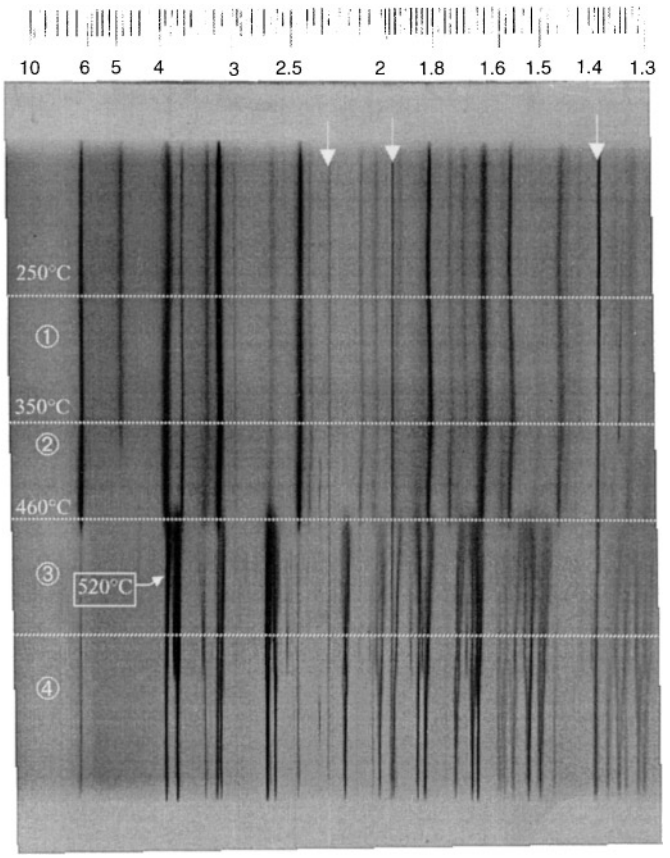

FIG. 2. Guinier–Lenne photograph of $H_{0.27}V_{0.27}W_{0.73}O_3 \cdot \frac{1}{3}H_2O$ (precursor) as a function of temperature. The platinum reflections (standards) are visible at $d = 2.27$, 1.96, and 1.39 Å.

of the diffraction lines due to structural transformations during heating of $H_{0.27}V_{0.27}W_{0.73}O_3 \cdot \frac{1}{3}H_2O$.

(1) Orthorhombic mixed vanadium–tungsten trioxide, $H_{0.27}V_{0.27}W_{0.73}O_3$. In the temperature region 250–350°C (Fig. 2), the displacements of the diffraction lines toward higher angles correspond to a decrease of the unit cell parameters without changing the orthorhombic crystal symmetry. The TG curve in Fig. 3 shows a weight loss during heating in air of the precursor, and the DTA curve shows a large endothermic peak centered at approximately 280°C. This peak indicates the loss of structural water ($0.33H_2O$) from the precursor. It is worth noting that the endothermic peak is followed by two exothermic peaks located at approximately 350 and 500°C. In the soft chemistry concept, an exothermic peak is characteristic of an irreversible phase transition between a metastable phase and a resulting more stable phase. By analogy with the work of Gerand *et al.* on the WO_3 system (2), the resulting product is in our case a supermetastable mixed oxide of approximate composition $H_{0.27}V_{0.27}W_{0.73}O_3$ which exists between 250 and 350°C and has a unit cell of orthorhombic symmetry with cell parameters close to those of the precursor.

(2) Hexagonal mixed vanadium–tungsten oxide, $H_{0.27}V_{0.27}W_{0.73}O_3$. The X-ray photograph in Fig. 2 shows that the supermetastable phase transforms at about 350°C to a metastable mixed oxide, which is isotypic with the hexagonal modification of WO_3. The refined unit cell dimensions, $a = 7.286(6)$ and $c = 3.8801(4)$ Å, are close to those previously given for WO_3(hex), $a = 7.298$ and 7.798 Å (10), except for the doubling of the c-axis which was obtained from an electron diffraction study.

The phase transition is characterized by the exothermic peak at 350°C on the DTA curve. The TG curve in Fig. 3 shows a small continuous weight loss during the transition up to approximately 500°C. It should be noted that thermogravimetric studies of the related hydrate $H_{0.33}V_{0.33}W_{0.67}O_3 \cdot \frac{1}{3}H_2O$ by Gopalakrishnan *et al.* (9) indicated that the weight loss took place in two steps. From our TG results it is clear that the starting material loses more than $0.33H_2O$. The excess can be due either to adsorbed water or to hydrogen combined with oxygen from the structure of the metastable $H_{0.27}V_{0.27}W_{0.73}O_3$ phase. The first case can be ruled out because we do not observe any change in the weight loss amplitude after an isothermal heat treatment of the precursor at 70°C for 10 hr. The composition of the mixed oxide $H_{0.27-x}V_{0.27}W_{0.73}O_{3-x/2}$ thus changes continuously through $0 \leq x < 0.27$, until the second phase transition occurs at 500°C.

(3) Monoclinic mixed vanadium–tungsten oxide, $V_{0.27}W_{0.73}O_{2.865}$. In the temperature region 500–600°C, the X-ray powder photograph in Fig. 2 shows that the metastable phase with a WO_3(hex)-related structure transforms irreversibly to a mixed oxide with a structure related to the monoclinic modification of WO_3. The reflections are diffuse, however, indicating a disordered structure. The unit cell dimensions of the new mixed oxide refined from the X-ray powder data are $a = 7.368(1)$ Å, $b = 7.500(1)$ Å, $c = 7.669(1)$ Å, and $\beta = 91.02(1)^\circ$. The corresponding values for WO_3(mon) are $a = 7.306$ Å, $b = 7.540$ Å, $c = 7.692$ Å, and $\beta = 90.88^\circ$ (5). The phase transition is characterized by an exothermic peak at 500°C in the DTA curve (Fig. 3), where the TG curve shows constant weight. The phase transition occurs in a narrow temperature region (50°C). The composition is $V_{0.27}W_{0.73}O_{2.865}$, obtained from the weight loss of the mixed hydrate. The formula indicates that both vanadium and tungsten adopt their highest oxidation states, V^{5+} and W^{6+}. The formula also suggests that there are vacancies in the ReO_3-type oxygen lattice. These vacancies are probably statistically distributed but it seems very likely that one oxygen is removed from between two vanadium atoms, as indicated by Fig. 1d. In this way the vanadium adopts a square pyramidal coordination.

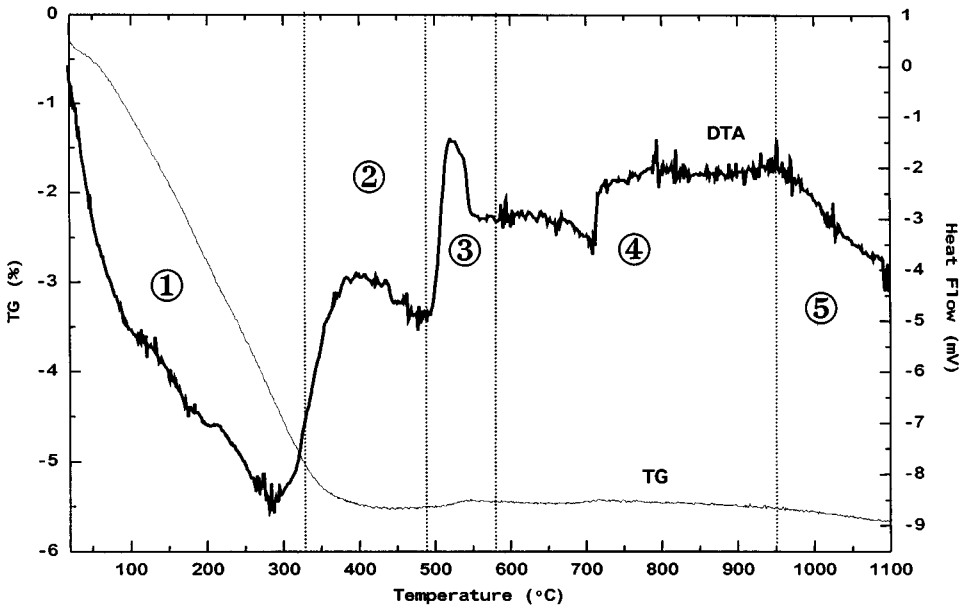

FIG. 3. Simultaneous thermal analysis (TG and DTA) of $H_{0.27}V_{0.27}W_{0.73}O_3 \cdot \frac{1}{3}H_2O$ preheated at 70°C for 10 hr.

A similar coordination polyhedron has been found in, for example, V_2O_5.

(4) Orthorhombic and tetragonal mixed vanadium–tungsten oxides of composition $V_{0.27}W_{0.73}O_{2.865}$. According to the X-ray diffraction pattern in Fig. 2, the crystal symmetry of $V_{0.27}W_{0.73}O_{2.865}$ increases above 600°C from monoclinic to orthorhombic to tetragonal. The phase transitions and the structures are complex, because they must involve displacements of the metal atoms in the polyhedra and tilting of the WO_6 octahedra and square VO_5 pyramids. In comparison with the WO_3 system, these phases are denoted high-temperature forms.

(B) HREM Study

(1) Phase transition between $H_{0.27}V_{0.27}W_{0.73}O_3 \cdot \frac{1}{3}H_2O$ ($WO_3 \cdot \frac{1}{3}H_2O$-type structure) and $H_{0.27}V_{0.27}W_{0.73}O_3$ (WO_3(hex)-related structure). The electron microscopy study showed that $H_{0.27}V_{0.27}W_{0.73}O_3 \cdot \frac{1}{3}H_2O$ forms agglomerates of thin hexagonal platelets, approximately 1000 Å in diameter. The dehydration was pseudomorphous as the particles of $H_{0.27}V_{0.27}W_{0.73}O_3$ retained the habitus (size, shape, and texture) of the starting material. The electron diffraction patterns taken of $H_{0.27}V_{0.27}W_{0.73}O_3 \cdot \frac{1}{3}H_2O$ showed that these particles lie on the (001) plane. It was difficult to obtain a monophasic electron microdiffraction pattern of the mixed oxide hydrate, as the dehydration of the phase occurred inside the microscope due to the high vacuum and heat from the electron beam. The SAED pattern in Fig. 4a exhibits reflections from both compounds. The rectangular arrangement of spots is typical of the hydrate phase with the orthorhombic unit cell, while the weaker spots in between, which give rise to a hexagonal spot pattern, clearly demonstrate the existence of $H_{0.27}V_{0.27}W_{0.73}O_3$ isotypic with WO_3(hex). It is thus possible to find the crystallographic relationships between the two phases: $[001]_{hydrate}//[001]_{hexagonal}$ and $[100]_{hydrate}//[100]_{hexagonal}$. The reaction is of a topotactic nature, with the same structural relationships as those previously observed in the WO_3 system (1).

The corresponding HREM image, shown in Fig. 4b, contains information about the coexistence of the two phases. First it should be noted that the black dots in the image correspond to projected columns of metal atoms in the structure. The rows of black dots marked by arrows in Fig. 4b are characteristic of the projected metal atoms in the rows of corner-sharing octahedra, which exist in both structures (Figs. 1a and 1b). From the arrangement of black spots between these rows, it should be possible to obtain information about the ordered and intergrowth structures. Rings of six black dots with a seventh in the middle are seen in the region marked 1 in Fig. 4b. This contrast is typical of the mixed oxide hydrate structure in Fig. 1a. In the area marked 2, six black dots are arranged in a ring with no black spot in the middle. This contrast is characteristic of the hexagonal tungsten bronze (HTB) related structure with empty six-sided tunnels as in the WO_3(hex) structure (Fig. 1b). In some regions (Fig. 4b, area marked 3), the intensity of the central

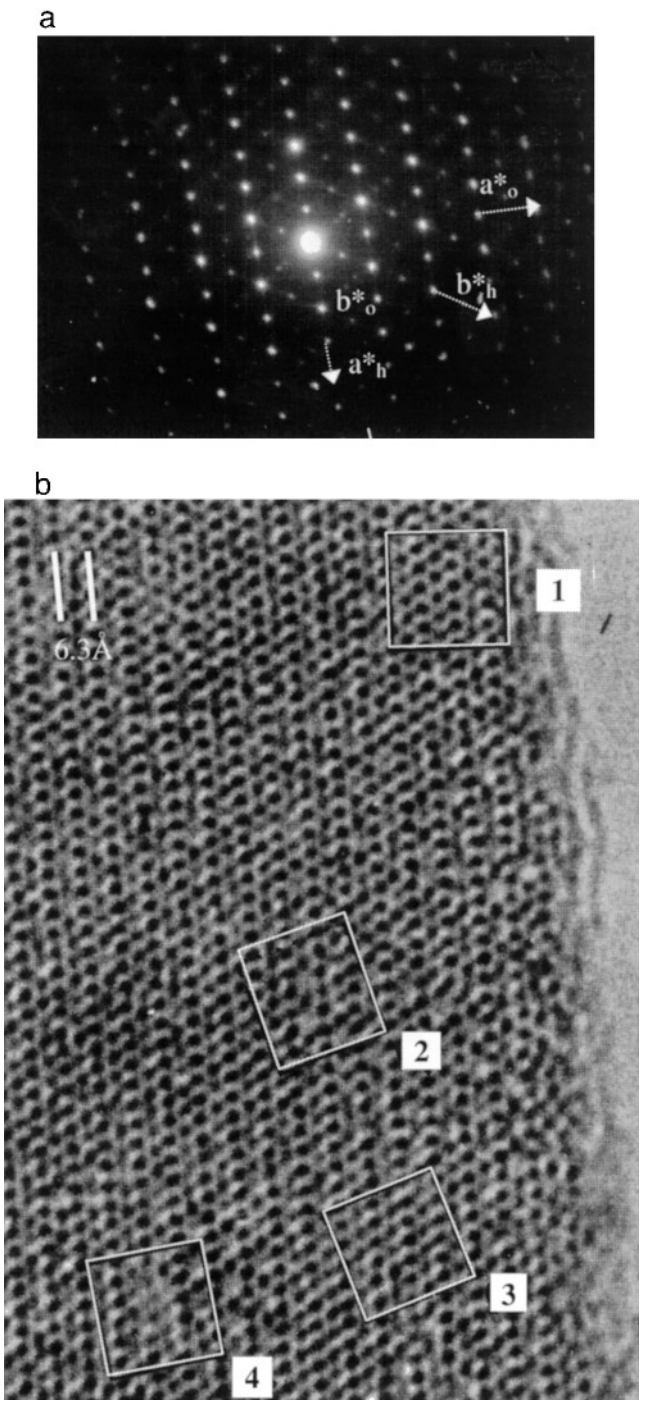

FIG. 4. (a) The SAED pattern shows reflections from both the hydrate and the $H_{0.27}V_{0.27}W_{0.73}O_3$(hex) phases. (b) Corresponding HREM image ([001] projection) showing that the phase transition is under way.

dot varies from one ring to the other. This change in contrast indicates that the transformation mechanism cannot be a simple shift of the layer of corner-sharing MO_6 octahedra ($M = V, W$) by $a/2$ in the hydrate structure, as suggested by the geometrical description of the structure. The change in contrast can be explained rather by displacement of some atoms along the tunnel rows. This displacement will give rise to tunnels along the *c*-axis, from half-filled in the hydrate phase (black dots) to empty ones in the WO_3(hex)-related phase (white dots), by going through all the intermediate steps (gray dots).

Another type of defect is visualized in the region marked 4. A few black dots in this area are almost absent (weak) in the rows representing the corner-sharing octahedra in the structures (see Figs. 1a and 1b). This contrast can be interpreted as being due to local evaporation of the crystal, resulting from irradiation damage by the heat from the electron beam. However, the examined crystal fragment seemed to be stable during the examination in the electron microscope. It thus seems more likely that the weaker dots indicate a local loss of surface atoms, creating a small hole in the crystal. This fault could then have been formed during the dehydration process. A possible explanation is that this contrast indicates the first step in the second phase transition from the hexagonal to monoclinic WO_3-related structure. During the latter transformation, holes of different sizes have been observed in HREM images (see following section). The creation of such holes seems to be involved in the transformation process and is also in agreement with the topochemical concept introduced by Figlarz (6).

(2) Phase transition between $H_{0.27}V_{0.27}W_{0.73}O_3$ (WO_3(hex)-related structure) and $V_{0.27}W_{0.73}O_3$ (WO_3(mon)-related structure). The initial hexagonal platelets of $H_{0.27}V_{0.27}W_{0.73}O_3$ lie on the (001) plane. During the phase transition from the hexagonal to monoclinic WO_3-related structure, pores appear and grow inside the crystals as shown in Fig. 5a. The reaction is not pseudomorphous. The HREM image in Fig. 5b, taken from a thicker part of a crystal, shows that the transformation process from the hexagonal to monoclinic structure is under way. A hole seems to be forming by local evaporation of the crystal. At the boundary of the HTB-related phase a regular arrangement of dark dots appears. This contrast is characteristic of a ReO_3-type structure and can thus be assigned to the $V_{0.27}W_{0.73}O_{2.865}$ phase. The SAED patterns in Fig. 6 are taken from different crystals, representing different stages in the transition process. The patterns contain reflection spots from both the hexagonal and the monoclinic structures. Most of the reflections in Fig. 6a are from the hexagonal phase, while the pattern in Fig. 6b shows that the ReO_3-type related structure is predominant in the latter crystal. The SAED patterns also show that the transformation is of a topotactic nature: $[001]_{hexagonal}//[001]_{monoclinic}$ and $[100]_{hexagonal}//[100]_{monoclinic}$. The HREM image in Fig. 7, corresponding to the SAED pattern in Fig. 6a, shows that the monoclinic phase (ReO_3-type structure) is formed on all three equivalent {1010}

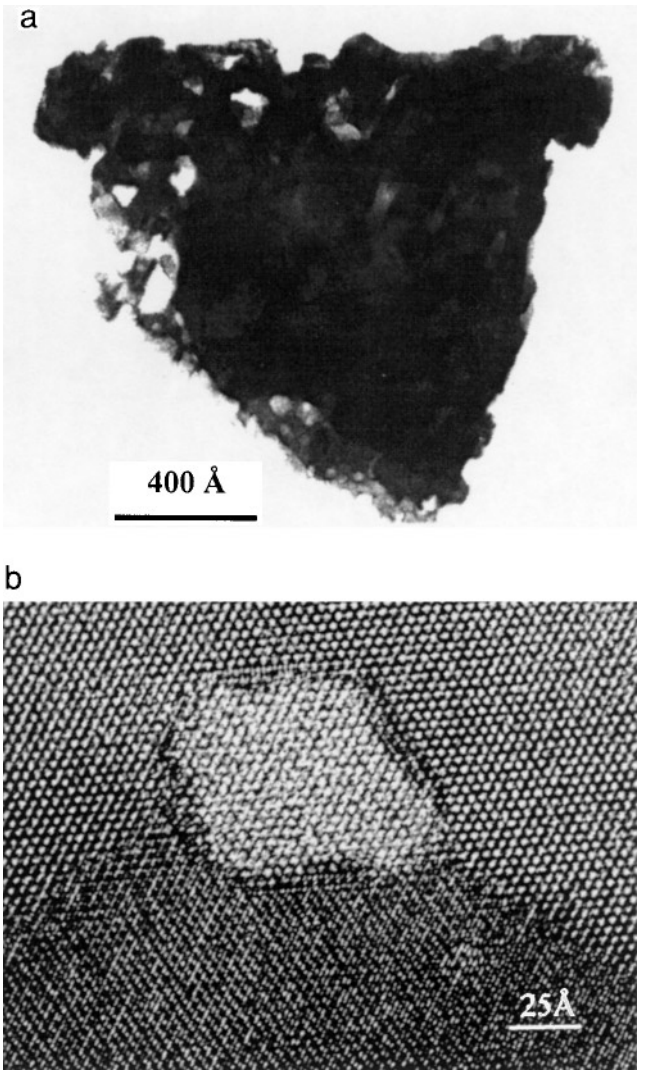

FIG. 5. (a) Low-magnification image showing holes in the crystal. (b) HREM image ([001] projection) showing an early stage of the phase transition $H_{0.27}V_{0.27}W_{0.73}O_3$(hex) → ReO_3-type structure.

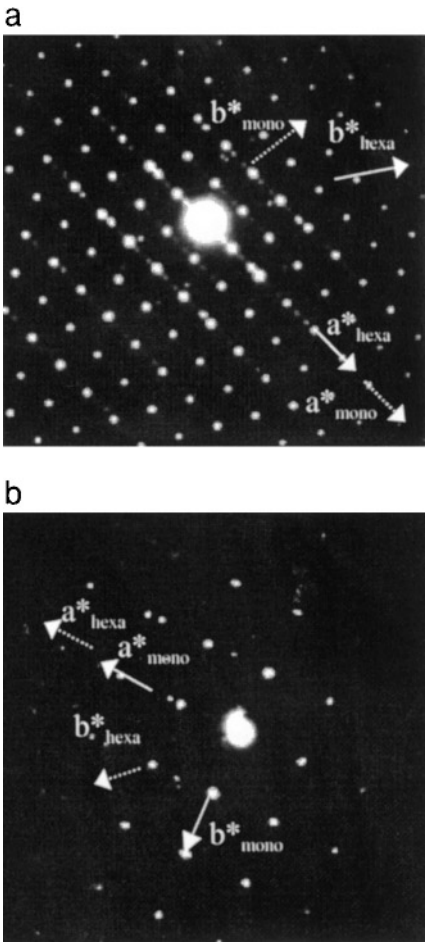

FIG. 6. Electron diffraction patterns showing two stages in the transformation process hexagonal → monoclinic WO_3-related phases. The predominant phase is (a) $H_{0.27}V_{0.27}W_{0.73}O_3$(hex) and (b) $V_{0.27}W_{0.73}O_{2.865}$(mon).

planes of the hexagonal phase. It should be noted that this phenomenon was not observed during the hexagonal → monoclinic WO_3 transition. The HREM image also shows that in some regions there is a good fit without discontinuity so that one row of octahedra belongs to both the hexagonal and the monoclinic structures. This is thus a coherent interface analogous to those previously observed in the WO_3 system. In other regions the boundary between the two phases is disordered, containing many faults. The HREM image in Fig. 8 shows that both pentagonal columns (11) and planar faults exist at the boundary between the hexagonal and monoclinic structures. The term pentagonal column represents a structural building unit, consisting of a pentagonal WO_7 bipyramid sharing edges with five corner-sharing WO_6 octahedra. These aggregates are joined by corner-sharing to form a column.

In the hexagonal region adjacent to the interface, the HREM image shows a dark dot in the middle of most of the six-sided tunnels. The dots are somewhat shifted from the central position, which could be due to a slight crystal tilt. There are also a couple of tunnels along the boundary which appear white, which are thus likely to be empty. It seems probable that the atoms have entered the six-sided tunnels during the evaporation process, leaving a hole in the crystal. On the basis of the HREM observations, we propose a mechanism for the nucleation and growth of the monoclinic phase. Hypothetical models of the proposed mechanism are summarized in Fig. 9.

(3) Proposed mechanism. Our results presented in the previous sections suggest that the protons in $H_{0.27}V_{0.27}W_{0.73}O_3$ stabilize the WO_3(hex)-related structure. Removal

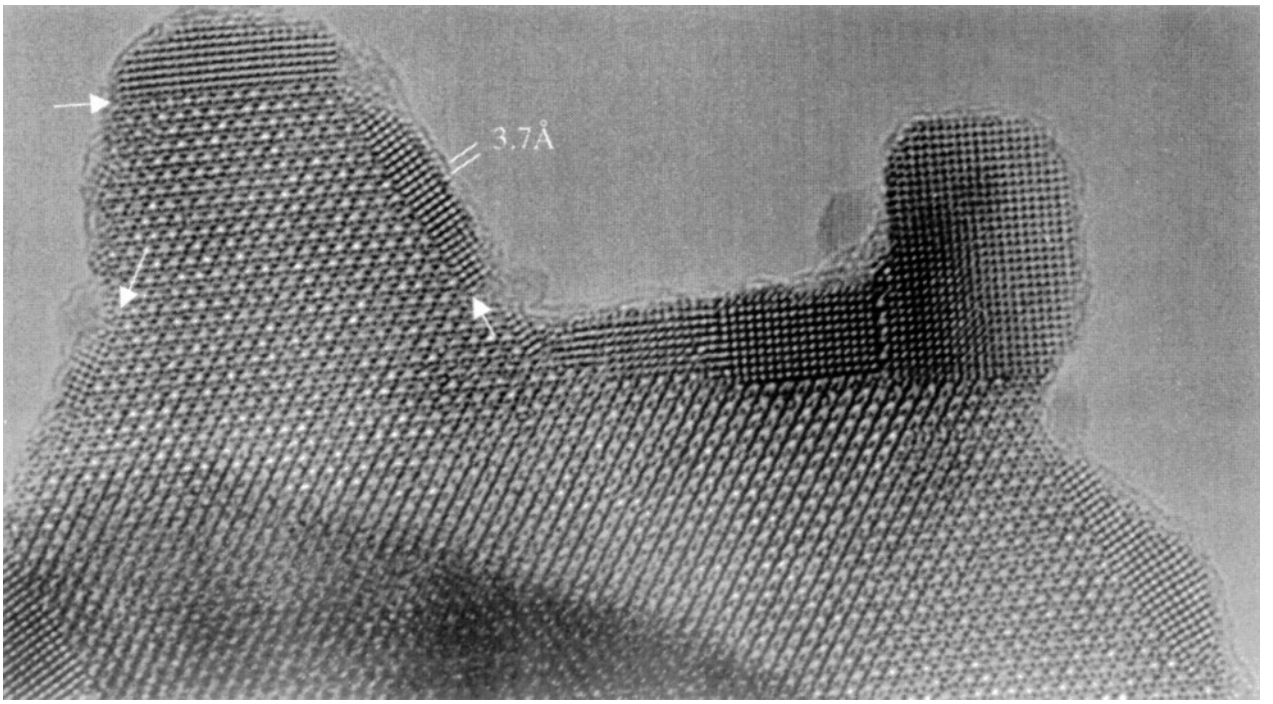

FIG. 7. HREM image ([001] projection) of a crystal with the corresponding SAED pattern in Fig. 6a.

of the hydrogen atoms by combination with oxygen atoms from the structure creates vacancies in the basic lattice. These vacancies might act as starting points for the evaporation process, resulting in the formation of holes in the crystals. We believe that by displacement of matter, the metal atoms move into the neighboring empty hexagonal tunnels, which may act as traps for the atoms. When the tunnels are sufficiently filled, a rearrangement takes place, involving small shifts of the metal and oxygen atoms, so that a new row of corner-sharing octahedra is formed. This row

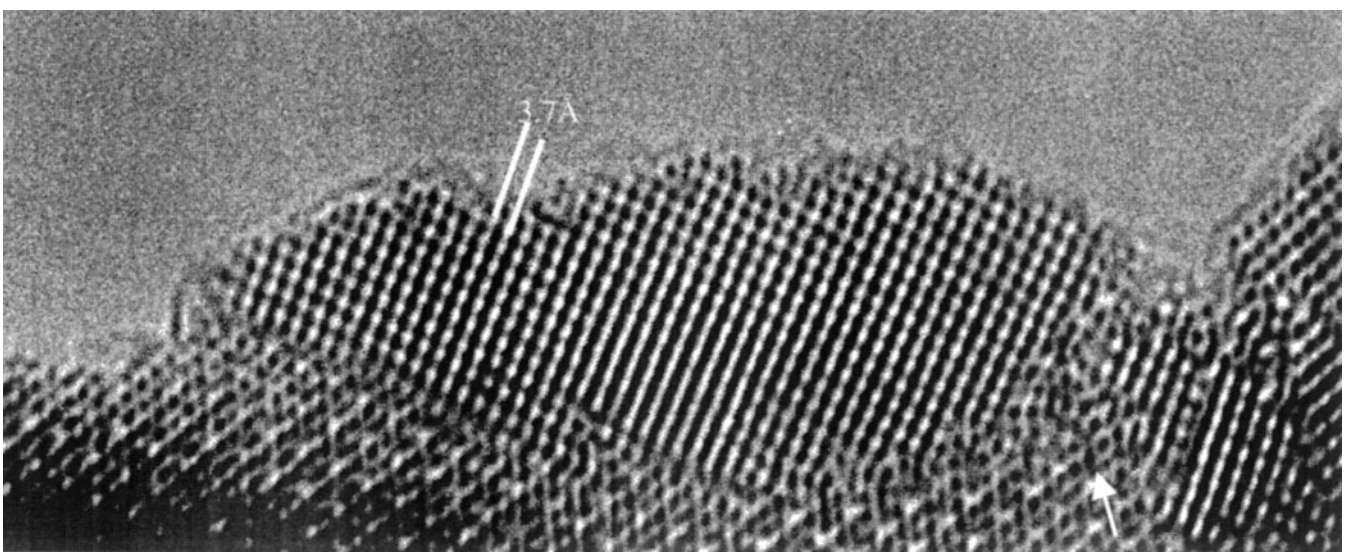

FIG. 8. HREM image showing defects in the boundary between the two WO_3-related phases. The arrow is pointing at a PC.

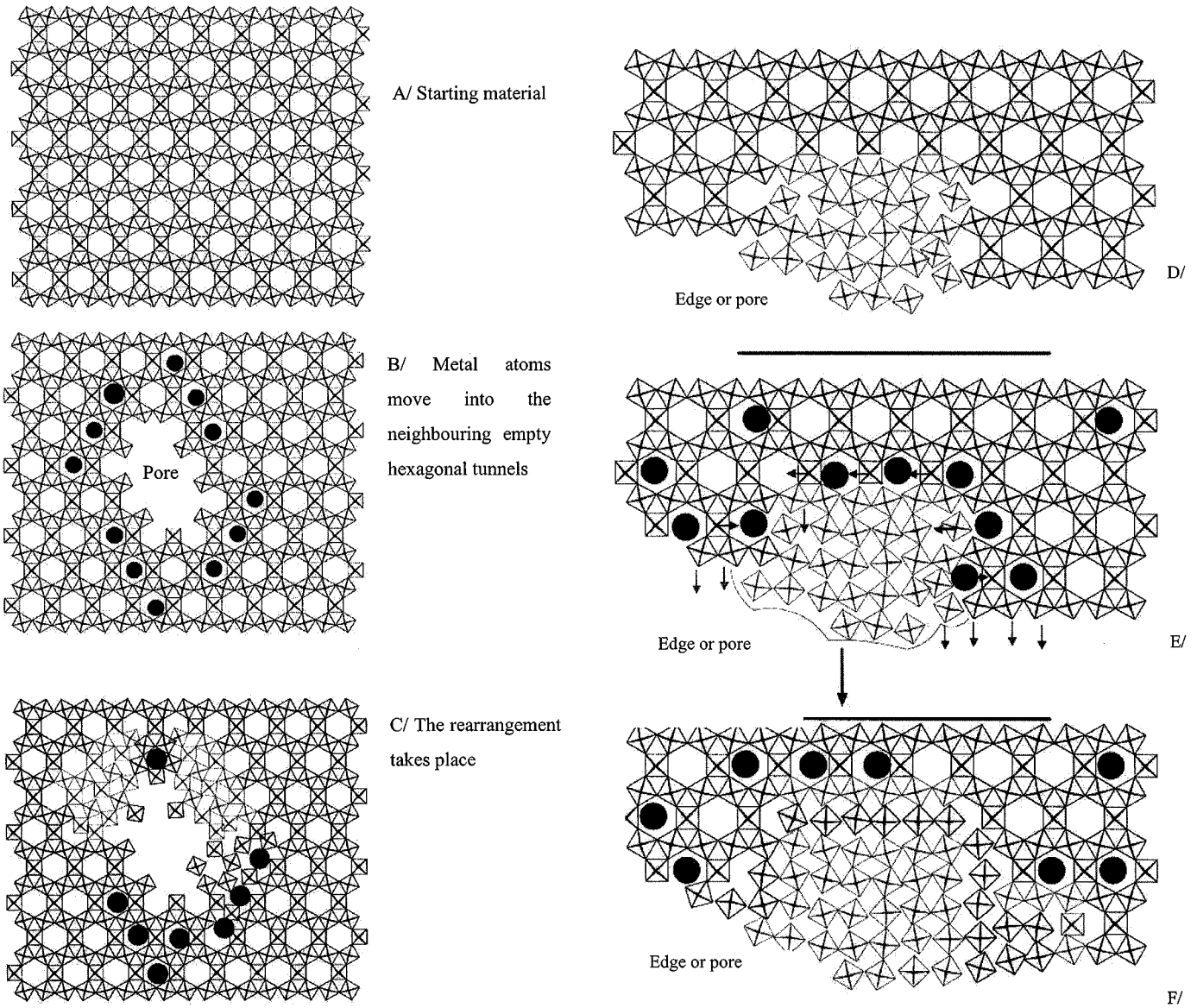

FIG. 9. Hypothetical models of the hexagonal → monoclinic phase transformation process. For simplicity, the models are drawn by using regular octahedra, which in most cases are assumed to be connected by corner-sharing. The black dots illustrate projected *M* atoms that have entered the six-sided tunnels during the evaporation process. (A) Basic lattice; (B–F) different stages during the transformation process.

will then link to the adjacent rows of octahedra in the hexagonal structure by sharing oxygen corners, thus forming the new monoclinic structure. The latter will expand, as can be seen in Fig. 9, causing strain in the crystal. The initial row of the hexagonal framework will become the coherent interface until a new row of the monoclinic phase is formed. The expansion of the monoclinic regions in the hexagonal structure occurs by additional filling of the hexagonal tunnels with supplementary atoms and subsequent shifts of the atoms near the interface. At the boundary between the regions, defects in the form of pentagonal columns are sometimes found. Previous observations made on defects in the intergrowth tungsten bronze structures show that HTB-tunnel rows often terminate in the WO_3(mon)-structure by forming a pentagonal column. This defect is coherently intergrown in the surroundings (12). At the end of the transition, there is no hexagonal phase left and the cavities are at maximum size. The strain inside the crystal can disappear and the rows of octahedra can become more and more linear as in the WO_3(mon) phase.

CONCLUDING REMARKS

We have shown that heating the precursor $H_{0.27}V_{0.27}W_{0.73}O_3 \cdot \frac{1}{3}H_2O$, isotypic with $WO_3 \cdot \frac{1}{3}H_2O$, first leads to the formation of a supermetastable oxide, $H_{0.27}V_{0.27}W_{0.73}O_3$, with a structure closely related to that of the hydrate. At 350°C the latter phase transforms to a metastable phase of the same composition, $H_{0.27}V_{0.27}W_{0.73}O_3$, isotypic with WO_3(hex). Our HREM studies show that the phase transformation is pseudomorphous and topotatic.

We can also conclude that the protons stabilize the metastable phase, as our results suggest that removal of hydrogen and oxygen, $H_{0.27-x}V_{0.27}W_{0.73}O_{3-x/2}$ $(0 \leq x < 0.27)$, transforms the metastable phase into more stable phases of composition $V_{0.27}W_{0.73}O_{2.865}$ at approximately 500°C. The structure of $V_{0.27}W_{0.73}O_{2.865}$ can be described as an oxygen-deficient WO_3(mon)-type structure. The symmetry increases to orthorhombic and then to tetragonal with increasing temperature. The HREM results show that the transition from the metastable phase with the WO_3(hex)-related structure to the more stable oxide with the WO_3(mon)-related structure is a nonpseudomorphous topotactic reconstructive transformation. During the reaction, the nucleation takes place equally well on all three equivalent planes of the hexagonal crystal. A hypothetical mechanism, based on the diffusion of matter, is proposed for the creation of pores and faults.

ACKNOWLEDGMENTS

The authors thank D. Larcher, F. Portemer, and B. Gerand for their scientific discussions. L.D. thanks the Department of Inorganic Chemistry, Stockholm University, for its hospitality and AREPIC for financial support. M.S. is grateful to the Swedish Natural Science Research Council for financial support.

REFERENCES

1. B. Gerand, G. Nowogrocki, and M. Figlarz, *J. Solid State Chem.* **38,** 312 (1981).
2. B. Gerand and L. Seguin, *Solid State lonics* **84,** 199 (1996).
3. M. Figlarz, *Solid State lonics* **43,** 143 (1990).
4. A. Magnéli, *Acta Chem. Scand.* **7,** 315 (1953).
5. B. O. Loopstra and H. M. Rietveld, *Acta Crystallogr., B* **25,** 1420 (1969).
6. M. Figlarz, *Rev. Chim. Miner.* **22,** 177 (1985).
7. M. Figlarz, B. Dumont, B. Gerand, and B. Beaudoin, *J. Microsc. Spectrosc. Electron.* **7,** 371 (1982).
8. L. Dupont, D. Larcher, F. Portemer, and M. Figlarz, *J. Solid State Chem.* **121,** 339 (1996).
9. J. Gopalakrishnan, N. S. P. Bhuvanesh, and A. R. Raju, *Chem. Mater.* **6,** 373 (1994).
10. B. Gerand, G. Nowogrocki, J. Guenot, and M. Figlarz, *J. Solid State Chem.* **29,** 429 (1979).
11. M. Lundberg, *Chem. Commun. Univ. Stockholm* **12,** 1–43 (1971).
12. L. Kihlborg, M. Sundberg, and A. Hussain, *Chem. Scr.* **15,** 182 (1980).